

Work Extraction and Landauer’s Principle in a Quantum Spin Hall Device

A. Mert Bozkurt,¹ Barış Pekerten,¹ and İnanç Adagideli^{1,*}

¹*Faculty of Engineering and Natural Sciences, Sabanci University, Orhanli-Tuzla, Istanbul, Turkey*

(Dated: June 16, 2022)

Landauer’s principle states that erasure of each bit of information in a system requires at least a unit of energy $k_B T \ln 2$ to be dissipated. In return, the blank bit may possibly be utilized to extract usable work of the amount $k_B T \ln 2$, in keeping with the second law of thermodynamics. While in principle any collection of spins can be utilized as information storage, energy/work extraction by utilizing this resource in principle requires specialized engines/machines that are capable of using this resource. In this work, we focus on heat and charge transport in a quantum spin Hall device in the presence of a spin bath. We show how a properly initialized spin bath can be used as a (Maxwell’s Demon memory) resource to induce charge current in the device that can power an applied external electrical load, using available heat energy from electrical reservoirs that couple to the device via electrical contacts. We also show how to initialize the spin bath using applied bias currents, that necessarily dissipate energy, hence demonstrating Landauer’s principle, as well as an alternative method of “energy storage” in an all electrical device. We finally propose a realistic setup to experimentally observe a Landauer erasure/work extraction cycle.

PACS numbers: 74.78.Na, 85.75.-d, 72.10.-d

According to Landauer’s principle, erasure of one bit of information requires an amount of heat greater than $k_B T \ln 2$ to be dissipated [1, 2]. The principle ensures that the second law of thermodynamics is obeyed as a blank bit is utilized to extract work by an amount $k_B T \ln 2$ from the environment. The “engine” that is capable of this extraction is sometimes called a “Maxwell’s Demon” (MD), referring to the thought experiment proposed by Maxwell in 1871 [3]. While interest in MD from the point of view of fundamental physics never faded [4–6], promise of highly efficient engines that operate in the nano-domain as well as alternative methods of energy storage gave a recent impetus to research on the physics of MD both experimentally (using colloidal particles [7–9], photonic systems [10, 11], NMR systems [12, 13], single electron transistors [14–16], cavity QED with superconducting qubits) [17] and theoretically [18–31]. Despite the multitudinous platforms in which MD action is theorized or demonstrated, scalability remains an issue.

In this manuscript, we propose and investigate a new MD implementation that harvests thermal energy from the electronic environment and converts it to electrical work using a quantum spin Hall insulator (QSHI). As a memory resource we use the available “spin bath” that usually includes the nuclear spins present in the device and/or magnetic impurities introduced via doping. QSHIs feature an insulating bulk and a pair of counter-propagating gapless spin-momentum locked helical edge states (HES) that are topologically protected from backscattering under time-reversal symmetry (TRS) [32] (see Figure 1). First predicted to occur in graphene nanoribbons [33, 34], they were later predicted and experimentally demonstrated in HgTe/CdTe quantum wells (QWs) [35, 36] as well as in InAs/GaSb QW structures [37, 38]. The TRS prohibiting the backscatter-

ing of the edge states is broken by the presence of nuclear or impurity spins. This backscattering shows up as extra dissipation, lowering the expected quantized conductance of the QSHI edge [39–43]. Here we show another salient feature of such scattering: an initial state of polarized nuclear spins (blank memory) drives an electrical current. Thus nuclear/impurity spins act as a memory resource of a MD that converts heat from the environment into electrical work.

We show below that for the heat harvesting operation of our engine, no energy exchange between nuclear and electronic systems is necessary; in fact, the nuclear spins are degenerate in our system, forming a non-energetic (pure) memory. Hence this is an alternative way for energy storage (Figure 2) that is protected from undesired explosive discharges. The total energy needed to reset the “memory” (or, in other words, recharge the device) by fully polarizing nuclear spins exceeds the extracted energy, in agreement with the second law of thermodynamics and Landauer’s principle. We also provide a method to generate such a nuclear spin polarization, completing the discharge-recharge cycle of the quantum information engine (QIE) (Figure 2). Note that each nucleus with nonzero nuclear spin coupling to the electron spin in the QSHE system contributes to the MD memory, hence the MD memory size here could be several orders of magnitude larger compared to those that were reported in the literature, thus solving the scaling problem for heat harvesting engines. Furthermore, our estimates show that equivalent energy/power density of our proposed engine compares favourably with conventional energy storage such as supercapacitors.

We now describe the basic operating principles of our MD implementation. The effective dynamics of electrons and holes in QSHI materials is well described by the

Bernevig-Hughes-Zhang (BHZ) Hamiltonian [35]:

$$\mathcal{H}_{\text{BHZ}} = \epsilon(k)\sigma_0\tau_z - Dk^2\sigma_0\tau_0 + A(k_x\sigma_z\tau_x - k_y\sigma_0\tau_y), \quad (1)$$

where $\epsilon(k) = M - Bk^2$ and M, B, D, A are the material parameters. Here $\sigma_i\tau_j \equiv \sigma_i \otimes \tau_j$ with σ_i and τ_j are the Pauli matrices corresponding to spin and electron-hole degrees of freedom respectively. In this description, the various two-dimensional QSHI QW structures differ only in their material and effective parameters [44], while the main edge state physics remains the same (Figure 1a). Next, we project the system into an effective edge Hamiltonian, obtaining $h_\beta^{\text{eff}} = -i\beta\hbar v_F\partial_x\sigma_z$ where $\beta = +1$ ($\beta = -1$) for the bottom (top) edge and v_F is the Fermi velocity of the effective edge state (Figure 1b). Note that in the presence of spin-orbit coupling, the spin axes becomes position dependent [45].

The second important element in our QIE is the nuclear spin subsystem that forms the ‘‘memory’’ of the MD that operates on electron-hole dynamics via their spins. We model the interaction between the spins of the nuclei and the spins of the electrons by the Fermi contact interaction. The total effective Hamiltonian including this interaction is then given by

$$H_\beta = -i\beta\hbar v_F\partial_x\sigma_z + \frac{\lambda}{2}M_z(x)\sigma_z$$

$$H_{\text{s-flip}} = \lambda \sum_{i=1}^N \delta(x - x_i)(I_{i+}\sigma_- + I_{i-}\sigma_+). \quad (2)$$

where $I_\pm\sigma_\mp = \sum_{i=1}^N \delta(x - x_i)I_{i\pm}\sigma_\mp$ is the spin-flip term with I_i being the spin operator of the i^{th} nucleus, $M_z(x)$ the Overhauser field and λ the hyperfine interaction strength [46]. Note that the Overhauser field merely moves the edge state in momentum space without causing any gap and can be gauged away via the unitary transformation $H_\beta \rightarrow UH_\beta U^\dagger$ with $U = \exp(i\frac{\beta\lambda}{2\hbar v_F} \int^x M_z(x')dx')$. For the sake of simplicity we assume the hyperfine interaction strength λ to be the same for each nuclear spin, which does not affect our overall results. We note that because the spin of the electron and its momentum is completely locked, as $H_{\text{s-flip}}$ flips the spin of the edge electron and one nuclear spin, it also causes backscattering (see Figure 1d). The Fermi contact interaction process runs in competition with other processes that affect the nuclear spins, mainly the quadrupole interaction causing spin-flip between nuclear spins. However, the rate of this interaction is orders of magnitude smaller than the coupling between nuclear and electronic spins [47].

We now describe the charging/discharging (or alternatively erasure/ work extraction) operation. In the charging phase, we apply a charge current, which without loss of generality we assume to be flowing to the left. Then there are more right movers than left movers

and hence more up(down) spins in the bottom(top) edge. Therefore, there is more right to left backscattering for both edges (see Figure 2a), increasing the number of up(down) nuclear spins for the bottom(top) edge. This process polarizes the nuclear spins until a certain net bias-dependent value is reached [39, 41]. This is the process of dynamical nuclear polarization for the quantum spin Hall edges, well-known in other contexts such as spin injection from ferromagnets [48, 49]. We stress that under a current bias, opposite edges are driven towards opposite polarization values.

More importantly, the reverse process is also possible: fully polarized nuclear spins near a QSH edge drive a charge current (see Figure 2b). This is the discharging phase. Consider a nonzero initial nuclear spin polarization (caused by, say, the driving current that was applied earlier, hence has opposite signs for opposite edges) and for the sake of simplicity assume zero applied voltage bias. Now there are more up(down)-nuclear spins than down(up)-nuclear spins in the bottom(top) edge, hence there are more down(up)-spins flipped to up(down)-spins in the bottom(top) edge leading to an imbalance of left movers relative to right movers. Any time a backscattering occurs, the event leaves its footprint via a spin-flip in the nuclear memory. A reverse bias can now be applied so that the current is opposite of the voltage bias in order to extract work. We show below that the energy is supplied by the thermal energy of the reservoirs. All this is reminiscent of a MD operation wherein the MD predominantly backscatters the right movers relative to the left movers, thus setting up a current between reservoirs that are otherwise in equilibrium, while recording the outcome in the nuclear spin memory(see Figure 2). Under applied reverse bias, the MD/QIE harvests heat to convert it to electrical work.

We now quantify our model. The spin-flip scattering rate at the edge can be calculated using Fermi’s golden rule. As mentioned above, all right(left) moving electrons have spin up(down) for the bottom edge (for the top edge all left(right) moving electrons have spin down(up)). From now on, without loss of generality, we focus on the bottom edge, where we denote the corresponding distribution functions by the subscript $+(-)$. Then the total rate for a single spin-flip scattering at a given energy, in which a right mover becomes a left mover by flipping a nuclear spin from down to up is given by [39, 41]:

$$\Gamma_{-+}(\epsilon) = \frac{\gamma_0}{\hbar} N_\downarrow f_+(\epsilon)(1 - f_-(\epsilon)), \quad (3)$$

where $\gamma_0 \equiv \lambda^2/8\pi\hbar^2 v_F^2$ is a dimensionless effective interaction strength for a single nuclear spin.

Nuclear polarization dynamics. The effect of spin-flip scattering on the nuclear spins is given by the rate equation:

$$\frac{dN_\uparrow}{dt} = \int d\epsilon (\Gamma_{-+}(\epsilon) - \Gamma_{+-}(\epsilon)). \quad (4)$$

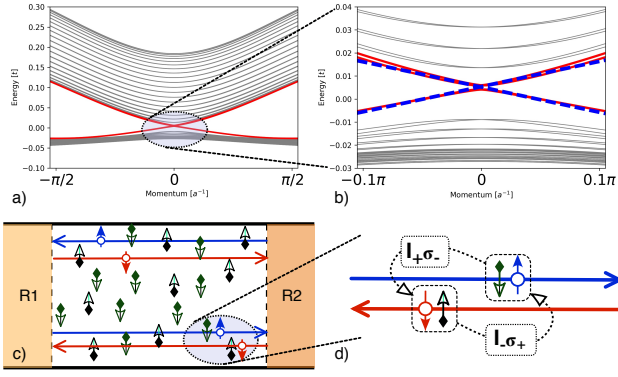


Figure 1. (Color online) The quantum spin Hall insulator with nuclear spins and electron-nuclear spin flip interaction. (a) The band structure of a typical QSHE nanowire system (using the BHZ model with tight-binding approximation). Red lines represent the edge states. (b) The band structure of the simplified Hamiltonian h_{eff} projected to a single edge (dashed blue lines). (c) Schematic description of the QSHE system with the edge currents interacting with the nuclear spins in the system, with the diamonds representing nuclear spins. (d) The spin flip interaction with the nuclear spins that form the Maxwell Demon.

We find it useful to define the mean polarization $m \equiv \frac{N_{\uparrow} - N_{\downarrow}}{2(N_{\uparrow} + N_{\downarrow})}$. Then, the rate of change of the mean polarization m is written as:

$$\frac{dm}{dt} = \gamma_0 \Gamma_B - m \gamma_0 \Gamma_T, \quad (5)$$

where

$$\begin{aligned} \Gamma_B &= \int \frac{d\epsilon}{\hbar} \frac{f_+ - f_-}{2}, \\ \Gamma_T &= \int \frac{d\epsilon}{\hbar} (f_+ + f_- - 2f_+ f_-). \end{aligned} \quad (6)$$

We assume a short edge (see below) and approximate the distributions f_{\pm}^0 by the Fermi distribution of the reservoir from which they originate. We then obtain $\hbar\Gamma_B = (\mu_L - \mu_R)/2$, and $\hbar\Gamma_T = (\mu_L - \mu_R) \coth(\frac{\mu_L - \mu_R}{2k_B T})$. Hence, using Eq. (5), the polarization dynamics is given by

$$m(t) = (m_0 - \bar{m})e^{-t/\tau_m} + \bar{m}, \quad (7)$$

where m_0 is the initial mean polarization and $\bar{m} \equiv \Gamma_B/\Gamma_T = (1/2) \tanh(\frac{\mu_L - \mu_R}{2k_B T})$ is defined to be the target mean polarization and $\tau_m = 1/\gamma_0 \Gamma_T$ is the characteristic time scale for nuclear polarization dynamics.

Electron dynamics and induced current. We now calculate the total current. The distribution functions obey the Boltzmann-like equation for the edge in consideration:

$$\partial_t f_{\pm} = \pm(\Gamma_{+-}(\epsilon) - \Gamma_{-+}(\epsilon)) \nu(0)^{-1} \mp v_F \partial_x f_{\pm},$$

where, $\nu(0) = L/2\pi\hbar v_F$ is the density of states of the edge electrons. We assume that the nuclear polarization

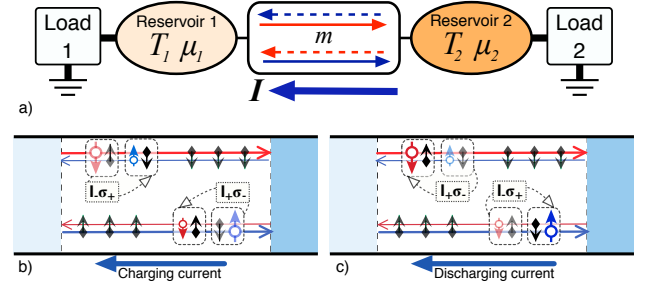


Figure 2. (Color online) a) QSH based quantum information engine, providing power to loads 1 and 2. Schematic description of b) the charging and c) the discharging phase of the QIE. In the charging phase, an applied bias current aligns the nuclear spins. In the discharging phase, flipping nuclear spins drive a current. An applied reverse bias can extract power.

m is changing slowly and seek a steady state solution. Then the distributions obey:

$$\partial_x f_{\pm} = (\Gamma_{+-}(\epsilon) - \Gamma_{-+}(\epsilon)) (v_F \nu(0))^{-1} \equiv \Gamma[f_+, f_-] \quad (8)$$

For short edges ($\Gamma L \ll 1$), we expand in gradients of the distribution functions. At the leading order, we obtain a linear position dependence:

$$f_{\pm} = f_{\pm}^0 + \Gamma[f_+, f_-^0](x \pm L/2), \quad (9)$$

where f_{\pm}^0 is the distribution of the left(right) reservoir. We then obtain the total current:

$$I_{\text{tot}} = \frac{e}{\hbar} \int d\epsilon (f_+ - f_-) = \frac{e^2}{\hbar} V - eN\gamma_0(\Gamma_B - m\Gamma_T). \quad (10)$$

We identify and focus on two sources of current in the system in the short edge regime: (i) the usual current $\frac{e^2}{\hbar} V$ due to voltage bias without the nuclear spin flip interaction, and (ii) the MD-induced current $-eN \frac{dm}{dt} = -eN\gamma_0(\Gamma_B - m\Gamma_T)$ due to the presence of nuclear polarization m . In the latter case, a net backscattering current, caused by right-moving up spin electrons scattering to left-moving down spin electron states, is driven by a net negative nuclear spin and vice versa. The net polarization of the nuclear spins acts as an MD.

We note that the total current is not zero for vanishing bias voltage, demonstrating the ‘‘Demon action’’ that induces a current between two reservoirs at equal temperature and chemical potential, while using the nuclear spins as a memory resource.

Generated power. In order to use the quantum information engine, we attach it to an electrical circuit as in Fig. 2. In this setup, the QIE provides power to loads 1 and 2, which can be modeled by a (reverse) bias voltage V . The power generated (Fig. 3) is given by:

$$P = \frac{eV}{\hbar} [eV(1 - \pi N\gamma_0) + 2\pi N\gamma_0 \hbar \Gamma_T m]. \quad (11)$$

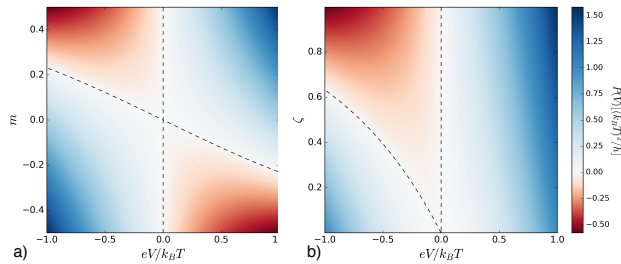


Figure 3. (Color online) P-V graph, calculated using Eq. 11, a) as a function of mean polarization m with $\zeta = 1.0$ and b) as a function of ζ with full polarization $m = 0.5$. On the dashed line, $P = 0$. Power can have negative values for $V < 0$ ($V > 0$) for a given mean polarization $m > 0$ ($m < 0$) (here, $e > 0$), as an indication of the work extraction phase.

For $eV < \frac{2\zeta\Gamma_T m}{(\zeta-2)}$, with $\zeta = 2\pi N\gamma_0$, we obtain $P < 0$, indicating the fact that the circuit is powered by the QIE. (For $eV > \frac{2\zeta\Gamma_T m}{(\zeta-2)}$, the circuit is providing power to charge the nuclear spin resource). We find the maximal work done by the nuclear spin resource in the weak coupling/short edge limit by maximizing the power and integrating up to the time when the power changes sign [50]:

$$W_{tot} = \alpha k_B T N^2 \gamma_0. \quad (12)$$

where α is a parameter of $\mathcal{O}(1)$ ($\alpha \sim \pi/4$ for a work extraction under constant voltage bias). In this limit, the amount of extracted work follows a quadratic scaling law that implies denser storage than the conventional/expected linear scaling. Here, T is the operating temperature, limited by the gap of the helical topological state in question.

We now discuss experimental feasibility of our MD implementation. Systems featuring spin-momentum locked topological edge states have been available to experiments for about a decade [51, 52]. Among these materials, systems with high nuclear spin density generally provide high energy density. In addition, systems with higher bulk bandgaps could be operated at higher temperatures, again leading to higher energy densities (see Eq. 12). Systems that feature high hyperfine interaction strength or low Fermi velocity provide high power density and fast operation, thus can be utilized as spin-supercapacitors. Assuming $N \sim 10^7$ and $\gamma_0 \sim 10^{-8}$, we estimate the equivalent energy density and power density that can be stored in the device in the short edge limit to be $\sim 10\text{kJ/kg}$ and $\sim 10\text{MW/kg}$ (not including overhead). On the other hand, systems with low interaction strength (see Eq. 3) due to high Fermi velocity and/or suppressed hyperfine interaction can be utilized as spin batteries that keep their polarization for long times. For example, thin film flakes of 3D topological QSH insulator $\text{Bi}_2\text{Te}_2\text{Se}$ (BTS221) feature a relatively large Fermi velocity ($v_F \sim 10^6\text{m/s}$) [53], which

is two orders of magnitude larger than that of, say, InAs/GaSb QWs ($v_F \sim 10^4\text{m/s}$) [38]. Thus, BTS221 features a much smaller electron-nuclear spin flip interaction strength (therefore requiring large currents to write the spin memory) and orders of magnitude longer memory retention times. In fact, recent experimental work that uses thin film flakes of BTS221 observed days long polarization retention times [54].

We next consider InAs/GaSb QW structures as an example. These QWs have a smaller Fermi velocity v_F [32, 38] and higher nuclear spin density compared to, for example, HgCdTe QWs [55]. This hints to a larger $N\gamma_0$ in InAs/GaSb QWs and therefore to a faster operation and higher energy density. We note that in these QWs, the electrons have spin $\pm 1/2$ but the holes have spin $\pm 3/2$ whose coupling to the spin flip interaction requires a higher order process [55]. The nuclear spin density in these QWs, as well as the effective electron spin–nuclear spin coupling strength, could possibly be further adjusted by magnetic impurity doping, providing a design freedom that might prove useful for different functionalities of the QIE.

In conclusion, we have described a Maxwell’s Demon system that utilizes the spin-flip interaction between helical edge states and nuclear spins in quantum spin Hall topological insulators. Available nuclear or magnetic impurity spins can be utilized as a Maxwell’s demon memory to harvest work from thermal energy of the reservoirs. We also showed how to erase the memory and thus “charge” the system by applying a voltage bias. Erasing the memory (or polarizing the spin subsystem) requires dissipation of heat by an amount at least $k_B T \ln 2$ per bit, in agreement with the Landauer’s principle and the second law. Estimates of equivalent work that can be extracted show that power/energy densities that exceed existing supercapacitors are achievable.

Acknowledgments — We especially thank N. Allen for inspiration as well as many fruitful discussions throughout this work. IA is a member of the Science Academy–Bilim Akademisi–Turkey; BP and AMB thank The Science Academy–Bilim Akademisi–Turkey for the use of their facilities. This research was supported by a Lockheed Martin Corporation Research Grant. IA and BP also acknowledge support by COST Action MP1209.

* adagideli@sabanciuniv.edu

- [1] R. Landauer, IBM J. Res. Devel. **3**, 183 (1961).
- [2] C. H. Bennett, Int. J. Theor. Phys. **21**, 905 (1982).
- [3] H. S. Leff and A. F. Rex, *Maxwell’s Demon 2* (IOP Publishing, Bristol, 2003); K. Maruyama, F. Nori and V. Vedral, Rev. Mod. Phys. **81**, 1 (2009).
- [4] S. Lloyd, Phys. Rev. A **56**, 3374 (1997).
- [5] M. O. Scully, Phys. Rev. Lett. **87**, 220601 (2001).
- [6] T. D. Kieu, Phys. Rev. Lett. **93**, 140403 (2004).

- [7] S. Toyabe, T. Sagawa, M. Ueda, E. Muneyuki and M. Sano, *Nat. Phys.* **6**, 988 (2010).
- [8] A. Berut, A. Arakelyan, A. Petrosyan, S. Ciliberto, R. Dillenschneider and E. Lutz, *Nature*, **483**,187-189 (2012).
- [9] É. Roldán, I. A. Martínez, J. M. R. Parrondo and D. Petrov, *Nature Phys.* **10**, 457 (2014).
- [10] M. D. Vidrighin, O. Dahlsten, M. Barbieri, M. S. Kim, V. Vedral and I. A. Walmsley, *Phys. Rev. Lett.* **116**, 050401 (2016).
- [11] M. A. Ciampini, L. Mancino, A. Orioux, C. Vigliar, P. Mataloni, M. Paternostro and M. Barbieri, *npj Quantum Inform.* **3**, Article number: 10 (2017).
- [12] P. A. Camati, J. P. S. Peterson, T. B. Batalhão, K. Micadei, A. M. Souza, R. S. Sarthour, I. S. Oliveira and R. M. Serra, *Phys. Rev. Lett.* **117**, 240502 (2016).
- [13] J. P. S. Peterson, R. S. Sarthour, A. M. Souza, I. S. Oliveira, J. Goold, K. Modi, D. O. Soares-Pinto and L. C. Céleri, *Proc. R. Soc. A* **472**, 2015.0813 (2016).
- [14] J. V. Koski, V. F. Maisi, T. Sagawa and J. P. Pekola, *Phys. Rev. Lett.* **113**, 030601 (2014).
- [15] J. V. Koski, V. F. Maisi, J. P. Pekola and D. V. Averin, *Proc. Natl. Acad. Sci. U.S.A.* **111**, 13786 (2014).
- [16] J. V. Koski, A. Kutvonen, I. M. Khaymovich, T. Ala-Nissila and J. P. Pekola, *Phys. Rev. Lett.* **115**, 260602 (2015).
- [17] N. Cottet, S. Jezouin, L. Bretheau, P. Campagne-Ibarcq, Q. Ficheux, J. Anders, A. Auffèves, R. Azouit, P. Rouchon and B. Huard, *arXiv:1702.05161* (2017).
- [18] S. Hilt, S. Shabbir, J. Anders and E. Lutz, *Phys. Rev. E* **83**, 030102(R) (2011).
- [19] A. C. Barato and U. Seifert, *Europhys. Lett.* **101**, 60001 (2013).
- [20] P. Strasberg, G. Schaller, T. Brandes and M. Esposito, *Phys. Rev. Lett.* **110**, 040601 (2013).
- [21] J. M. Horowitz, T. Sagawa and J. M. R. Parrondo, *Phys. Rev. Lett.* **111**, 010602 (2013).
- [22] D. Mandal, H. T. Quan and C. Jarzynski, *Phys. Rev. Lett.* **111**, 030602 (2013).
- [23] S. Deffner, *Phys. Rev. E* **88**, 062128 (2013).
- [24] J. J. Park, K. H. Kim, T. Sagawa and S. W. Kim, *Phys. Rev. Lett.* **111**, 230402 (2013).
- [25] J. Roßnagel, O. Abah, F. Schmidt-Kaler, K. Singer, and E. Lutz, *Phys. Rev. Lett.* **112**, 030602 (2014).
- [26] J. Gemmer and J. Anders, *New J. Phys.* **17** 085006 (2015).
- [27] J. P. Pekola, D. S. Golubev and D. V. Averin, *Phys. Rev. B* **93**, 024501 (2016).
- [28] A. Kutvonen, J. Koski and T. Ala-Nissila, *Scientific Reports*, vol 6 , 21126 , pp. 1-7 (2016).
- [29] M. Campisi, J. Pekola, R. Fazio, *arXiv:1702.05604* (2017).
- [30] C. Elouard, D. Herrera-Martí, B. Huard, A. Auffèves, *arXiv:1702.01917* (2017).
- [31] G. Rosselló, R. López, G. Platero, *arXiv:1703.03221* (2017).
- [32] M. König, H. Buhmann, L. W. Molenkamp, T. L. Hughes, C.-X. Liu, X.-L. Qi, and S.-C. Zhang, *J. Phys. Soc. Jpn* **77**, 031007 (2008).
- [33] C. L. Kane and E. J. Mele, *Phys. Rev. Lett.* **95**, 146802 (2005).
- [34] C. L. Kane and E. J. Mele, *Phys. Rev. Lett.* **95**, 226801 (2005).
- [35] B. A. Bernevig, T. L. Hughes, S.-C. Zhang, *Science* **314**, 1757-1761 (2006).
- [36] M. König, S. Wiedmann, C. Brune, A. Roth, H. Buhmann, L. W. Molenkamp, X.-L. Qi, and S.-C. Zhang, *Science* **318**, 766 (2007).
- [37] C. Liu, T.L. Hughes, X.-L. Qi, K. Wang and S.-C. Zhang, *Phys. Rev. Lett.* **100**, 236601 (2008).
- [38] L. Du, I. Knez, G. Sullivan and R.-R. Du, *Phys. Rev. Lett.* **114**, 096802 (2015).
- [39] A. M. Lunde and G. Platero, *Phys. Rev. B* **86**, 035112 (2012).
- [40] V. Cheianov and L. I. Glazman, *Phys. Rev. Lett.* **110**, 206803 (2013).
- [41] A. Del Maestro, T. Hyart, and B. Rosenow, *Phys. Rev. B* **87**, 165440 (2013).
- [42] L. Kimme, B. Rosenow, and A. Brataas, *Phys. Rev. B* **93**, 081301(R) (2016).
- [43] Ch.-H. Hsu, P. Stano, J. Klinovaja, D. Loss, *arXiv:1703.03421* (2017).
- [44] C. Liu and S.-C. Zhang, *Models and materials for topological insulators*. In: *Topological Insulators*. Elsevier, 2013, p.59-86.
- [45] I. Adagideli, V. Lutsker, M. Scheid, Ph. Jacquod and K. Richter, *Phys. Rev. Lett.* **108** 236601 (2012).
- [46] C. Slichter, *Principles of Magnetic Resonance*, Spinger Series in Solid-State Sciences (Springer, Berlin, 1990).
- [47] R. I. Dzhioev and V. L. Korenev , *Phys. Rev. Lett.* **99**, 037401 (2007).
- [48] S. Datta and B. Das, *Appl. Phys. Lett.* **56**, 665 (1990).
- [49] G. Schmidt, D. Ferrand, L. W. Molenkamp, A. T. Filip, and B. J. van Wees, *Phys. Rev. B* **62**, R4790(R), (2000).
- [50] We note that the time it takes to complete the charge/discharge cycle is only limited by the time it takes for an edge-resolved nuclear spin polarization to relax via spin-flip between nuclear spins. Nuclear spin polarization in similar systems have been reported to hold for days [54].
- [51] M. Z. Hasan and C. L. Kane, *Rev. Mod. Phys.* **82**, 3045 (2010).
- [52] X. L. Qi and S. C. Zhang, *Rev. Mod. Phys.* **83**, 1057 (2011).
- [53] S.-Y. Xu, L. A. Wray, Y. Xia, R. Shankar, A. Petersen, A. Fedorov, H. Lin, A. Bansil, Y. S. Hor, D. Grauer, R. J. Cava, M. Z. Hasan, *arXiv:1007.5111* (2010).
- [54] J. Tian, S. Hong, I. Miotkowski, S Datta, Y. P. Chen, *Sci. Adv.* **3**, e1602531 (2017).
- [55] A. M. Lunde and G. Platero, *arXiv:1304.5096v2* (2013).

Appendix

In this section, we calculate the power and work extracted from the system. The power extracted under bias is given by

$$\begin{aligned}
 P(t) &= \frac{eV}{h} \left[eV \left(1 - \frac{\zeta}{2}\right) + \zeta m(t) \hbar \Gamma_T \right], \\
 &= \frac{eV}{h} \left[eV \left(1 - \frac{\zeta}{2}\right) + \zeta (m_0 - \bar{m}) e^{-t/\tau_m} \hbar \Gamma_T + \zeta \bar{m} \hbar \Gamma_T \right].
 \end{aligned}
 \tag{13}$$

Rearranging the above equation and substituting $\bar{m}\hbar\Gamma_T = \frac{eV}{2}$, we obtain

$$P(t) = \frac{eV}{h} \left[eV + \zeta(m_0 - \bar{m})e^{-t/\tau_m} \hbar\Gamma_T \right]. \quad (14)$$

Charging cycle: We would like to find the heat dissipated while we charge the device. Starting from totally unpolarized nuclear spins ($m_0 = 0$) and using Eqn. (15), we get:

$$\begin{aligned} P(t) &= \frac{eV_C}{h} \left[eV_C - \zeta\bar{m}e^{-t/\tau_m} \hbar\Gamma_T \right], \\ &= \frac{eV_C}{h} \left[eV_C - eV_C \frac{\zeta}{2} e^{-t/\tau_m} \right]. \end{aligned} \quad (15)$$

As seen in Eq. (7), one has to wait infinitely long amount of time to reach the target mean polarization. Instead, we charge the device up to a fraction of full polarization $m = \frac{\kappa}{2}$ where κ is a value we later choose to maximize power or efficiency depending on the application. We then calculate the amount of time, \bar{t} , to reach the specified target mean polarization using $\frac{\kappa}{2} = \bar{m}(1 - e^{-\bar{t}/\tau_m})$ and obtain:

$$\bar{t} = -\tau_m \ln \left(1 - \frac{\kappa}{2\bar{m}} \right). \quad (16)$$

We then get the heat dissipated by integrating the power up to \bar{t} :

$$\begin{aligned} W_C(V_C) &= \int_0^{\bar{t}} \frac{eV_C}{h} \left[eV_C - \frac{\zeta}{2} e^{-t/\tau_m} eV \right], \\ &= \frac{e^2 V_C^2}{h} \tau_m \left[-\ln \left(1 - \frac{\kappa}{2\bar{m}} \right) - \frac{\zeta}{2} \frac{\kappa}{2\bar{m}} \right], \\ &= \frac{eV_C}{2\pi\gamma_0} \tanh \left(\frac{eV_C}{2k_B T} \right) \left[\ln \left(\frac{2\bar{m}}{2\bar{m} - \kappa} \right) - \frac{\zeta}{2} \frac{\kappa}{2\bar{m}} \right]. \end{aligned} \quad (17)$$

Note that $0 \leq 1 - \kappa/2\bar{m} < 1$, and this condition gives us an lower bound on the voltage applied as:

$$V_C \geq \frac{k_B T}{e} \ln \left(\frac{1 + \kappa}{1 - \kappa} \right). \quad (18)$$

Discharging cycle: As a next step in the cycle, we apply a reverse bias, $V_D < 0$, and we would like to find the time

t^* at which $P(t)$ changes sign, i.e. $P(t^*) = 0$. Using Eqn. (15), we obtain:

$$\begin{aligned} -|eV_D| &= \zeta\hbar\Gamma_T(\bar{m} - m_0)e^{-t^*/\tau_m}, \\ |eV_D| &= \zeta e^{-t^*/\tau_m} \left(\frac{|eV_D|}{2} + m_0 |eV| \coth \left(\frac{eV_D}{2k_B T} \right) \right), \\ t^* &= \tau_m \ln \left[\zeta \left(\frac{1}{2} + m_0 \coth \left(\frac{eV_D}{2k_B T} \right) \right) \right] \end{aligned} \quad (19)$$

We then integrate the power up to $t = t^*$ to obtain the work done at fixed voltage:

$$\begin{aligned} W_D(V_D) &= \int_0^{t^*} \frac{|eV_D|}{h} \left[|eV_D| - \zeta(m_0 - \bar{m})e^{-t/\tau_m} \hbar\Gamma_T \right], \\ &= \frac{e^2 V_D^2}{h} t + \frac{|eV_D|}{h} \tau_m \zeta(m_0 - \bar{m}) \hbar\Gamma_T e^{-t/\tau_m} \Big|_0^{t^*}, \\ &= \frac{e^2 V_D^2}{h} t^* + \frac{|eV_D|}{h} \tau_m \zeta(m_0 - \bar{m}) \hbar\Gamma_T (e^{-t^*/\tau_m} - 1). \end{aligned} \quad (20)$$

Inserting t^* into the equation above and using the relation $\bar{m}\hbar\Gamma_T = -\frac{|eV_D|}{2}$, we get:

$$\begin{aligned} W_D(V_D) &= \frac{e^2 V_D^2}{h} \tau_m \left[\ln \left(\zeta \left(\frac{1}{2} + m_0 \coth \left(\frac{|eV_D|}{2k_B T} \right) \right) \right) \right. \\ &\quad \left. + 1 - \zeta \left(\frac{1}{2} + m_0 \coth \left(\frac{|eV_D|}{2k_B T} \right) \right) \right]. \end{aligned} \quad (21)$$

We finally take the polarization reached at the end of the charging cycle, $m_0 = \frac{\kappa}{2}$, as the initial polarization for discharging to finally obtain

$$\begin{aligned} W_D(V_D) &= \frac{|eV_D|}{2\pi\gamma_0} \tanh \left(\frac{|eV_D|}{2k_B T} \right) \left[\ln \left(\frac{\zeta}{2} \left(1 + \kappa \coth \left(\frac{|eV_D|}{2k_B T} \right) \right) \right) \right. \\ &\quad \left. + 1 - \frac{\zeta}{2} \left(1 + \kappa \coth \left(\frac{|eV_D|}{2k_B T} \right) \right) \right]. \end{aligned} \quad (22)$$

In order to extract work from the nuclear spin polarization, one has to make sure that $t^* > 0$, which gives us an upper bound on the applied voltage as:

$$|V_D| \leq \frac{k_B T}{e} \ln \left(\frac{2 - \zeta(1 - \kappa)}{2 - \zeta(1 + \kappa)} \right). \quad (23)$$